J. Condensed Matter Nucl. Sci. 38 (2024) 51–77

Research Article

Energetic Ion Emission from TiD_x in Low-Energy Ion Beam Experiments

Sadie Forbes, Peter L. Hagelstein and Florian Metzler

Massachusetts Institute of Technology, Cambridge, MA, USA

Abstract

Low-level energetic ion emission has been reported previously in many low-energy nuclear reactions (LENR) experiments including electrolysis, gas-loading and ion beam experiments. The corresponding reports present evidence for MeV-level charged ions and neutrons associated with deuterium-deuterium fusion reactions, and also particles at higher energy that would be expected to originate from other processes. A study of low-level energetic nuclear particles has the potential to shed light on nuclear processes relevant to excess heat production and other LENR anomalies, which provides motivation to focus on such observables. In some of the referenced earlier experiments a small number of very energetic charged particle emissions near 20 MeV have been reported, which is of particular interest to us in connection with the involved mechanisms. We developed an ion beam experiment in which thick (1.59 mm) and thin (5 μm) Ti foils were initially loaded with deuterium by ion beam implantation and then bombarded with argon ions at 950 eV. A small number of counts in high-energy detector channels were recorded in eight different experiments, corresponding to particle energies estimated to be between 32-40 MeV, based on a calibration at lower energies with an ^{241}Am calibration source. Experiments with the 5 μm Ti foil also resulted in dozens of counts below about 11 MeV.

Keywords: Ion Emission, LENR, Charges Particles, Beam Experiments

1. Introduction

In the early days of research on low-energy nuclear reactions (LENR), many approaches were used to load palladium and other metals with deuterium including electrochemistry and gas loading, as well as loading with ion beams. A perceived advantage of ion beam implantation was that it was potentially possible to develop a D/Pd loading in excess of unity, especially at low temperature where deuterium diffusion is inhibited [1]. Early experiments done at Sandia National Laboratories [2], [3], and at the United States Naval Research Laboratory (NRL) [4] showed no anomalies, even under conditions with very high D/Pd loading ratios. Electron screening of dd-fusion reactions has been studied using accelerators at low energy, where evidence for anomalously large screening energies has been obtained [5]–[10].

There have been reports of LENR anomalies in ion beam experiments. Low-level charged particle emission near 20 MeV was reported from D implantation in PdD_x in [11]. A charged particle peak near 5 MeV was observed from D bombardment of TiD_x [12], [13]. And a small number of charged particles were seen near 8.6 MeV in ion beam experiments with proton bombardment of Li [14].

We obtained support to explore potential alpha particle emission from proton bombardment of Li, motivated by claims of p+^{7}Li fusion in glow discharge experiments by Lipinski and Lipinski [15], [16]. However, the planned campaign was interrupted by the Covid-19 pandemic, before all equipment was fully operational. In light of the positive result reported in [14] we would like to resume this campaign in the future.

In initial exploratory experiments (herein referred to as the "2019 experiments") with the ion beam experimental setup, we conducted some runs with D implantation of Ti, which resulted in several counts of interest with a charged particle detector and with a neutron detector (as discussed below in this article). In more recent experiments that sought to build on those initial findings (the "2022 experiments"), we have observed more counts of interest from TiD_x, all of which has provided motivation for documenting the experimental work to date in this article. We recognize that the presented results to date can be—and should be—improved in many ways. The purpose of this article is to share the experimental work that has been conducted thus far, to discuss the issues that have emerged, to share lessons learned, and to lay out plans for the continuation of this work.

There are quite a few issues to be considered in connection with ion beam based LENR experiments. One experimental issue concerns the lack of reproducibility associated with earlier ion beam experiments, and the need to develop a protocol that can result in comparatively high degrees of reproducibility of reported anomalies. In our recent experiments, low-level energetic ion emission is observed with an improved degree of reproducibility over earlier experiments; however, there is much room for further improvement. Another issue concerns the origins of the observed effect, and the question more generally of whether and how charged particle emission from metal deuterides may occur in LENR experiments. Related to this is the identification of the particles emitted, as well as the precise characterization of the particle energy. Looming large is the question of the origin of the energetic particles, and what conditions are required to produce them. In the remainder of this article, we will engage with these questions in the context of presenting data from the 2019 and 2022 experiments with TiD_x. We will begin with a brief review of related reports in the literature.

2. Brief Review of Reports of Low-level MeV Nuclear Product Emissions in LENR Experiments

The majority of LENR experiments over the years have focused on excess heat measurements, which would be the biggest effect in terms of corresponding reaction rates, and which may eventually lead to commercial applications. There have been fewer experiments that focus on low-level nuclear emissions. In this section, we discuss past LENR experiments, in which neutron spectra were observed and recorded, and in which charged particle spectra were observed and recorded (and in some cases particle identification carried out).

2.1. Low-level Neutron Spectra

Recall that following the announcements of 1989 by Fleischmann and Pons a great deal of work was done by many research groups around the world looking for nuclear signatures from metal deuterides, and most of the results were negative. A small subset of experiments, in which low-level neutron emission was sought and not observed, are documented in [17]–[26]. The large number of negative results published at the time has been interpreted by many as proof that there are no nuclear anomalies in metal deuterides—an interpretation that is, however, not in agreement with other publications. A better interpretation is that for one reason or another, these groups were not able to reproduce earlier claimed experimental results due to a lack of understanding of the experiments and conditions needed to obtain such results.

Even with imperfect reproducibility (as in the Frascati experiment, where TiD is cycled in gas), it has been possible to detect low-level neutron emission, and also to accumulate spectral information. A summary of published results, in which spectral information was obtained is given in Table 1. Most of the neutron spectral measurements on LENR experiments are consistent with 2.45 MeV emission from the reaction

Table 1. LENR experiments with reported neutron spectra. Note that the metal deuterides are indicated generically in the form of MeD, without an attempt to indicate specific loadings reported.

Author	Year	Ref.	MeD	Type	Detector	Peaks (MeV)
Jones	1989	[27]	TiD	electrolysis	BC-505 recoil	2.5
Bertin	1989	[28]	TiD	electrolysis	NE-213 recoil	2.5
Shani	1989	[29]	PdD	gas loading	NE-213 recoil	2.5
Wolf	1990	[30]	TiD,PdD	electrolysis, gas	NE-213 recoil	2.5
Takahashi	1990	[31]	PdD	electrolysis	NE-213 recoil	2.45,4.5,7
Bressani	1991	[32]	TiD	cycling in gas	NE-110 TOF	2.5
Bressani	1991	[33]	TiD	cycling in gas	NE-110 TOF	2.5
Takagi	1991	[34]	PdD	electrolysis	NE-110 TOF	2.5
Takahashi	1991	[35]	PdD	electrolysis	NE-213 recoil	2.45,4.5,6
Botta	1992	[36]	TiD,PdD	cycling in gas	NE-110 TOF	2.5 and above
Nakada	1993	[37]	PdD	electrolysis	NE-213 recoil	2.45, 3-7
Bittner	1993	[38]	PdD	electrolysis, degassing	NE-213 recoil	2.5
Long	1993	[39]	many	glow discharge	recoil	up to 10.5
Lipson	2000	[40]	Au/PdD/PdO	electrolysis	NE-213, recoil	2.5
Steinetz	2020	[41]	TiD,ErD	gas-loading, x-ray	EJ-309, others	2.45, 4-5

$$\mathrm{d + d \rightarrow n(2.4497\ MeV) + {}^{3}He(0.8193\ MeV)}$$

In all of these papers, evidence for emission near 2.5 MeV is reported, consistent with dd-fusion. We draw attention to the fact that in some cases, significant emission is reported at higher energies, indicative of nuclear processes other than dd-fusion. The early measurements of Takahashi et al. [31], [35] are particularly relevant in this regard. We have chosen to include the recent NASA experiment [41] as a LENR experiment closely related to earlier experiments, recognizing that not all would agree with such an interpretation.

Note that CR-39 has been used for the detection of energetic neutrons above 9.6 MeV, where the neutron energy can be inferred from triple tracks that result from ^{12}C(n,n′)3α carbon breakup [42]–[45].

2.2. Low-level Charged Ion Spectra

Also following the 1989 announcements by Fleischmann and Pons, experiments were conducted seeking charged particle emission in LENR experiments, in which, however, no evidence for anomalous charged particles was found [46]–[48]. A conclusion is that simply loading deuterium into a metal does not guarantee that reported LENR effects can be observed.

The observation of low-level neutron emission in LENR experiments near 2.5 MeV would suggest that there should also be a charged particle emission effect based on the 0.82 MeV ^{3}He from the n+^{3}He dd-fusion channel, as well as from the other main dd-fusion channel

$$\mathrm{d + d \rightarrow p(3.0226\ MeV) + t(1.0100\ MeV)}$$

In an experiment by Jones and coworkers [49] with TiD, protons were observed near 2.6 MeV based on dE-E measurements with plastic and glass scintillators. Also described is a coincidence experiment, in which samples were placed between two large-area silicon charged particle detectors, and coincidence measurements were done for protons and tritons of this branch of the dd-fusion reaction.

A list of publications, in which charged particle spectral information is reported, is presented in Table 2. Low-level charged ion emission in these experiments appears to be a weak effect, and the number of reported counts tends to be small. Nevertheless, counts are seen both with active detectors (silicon and diamond-based) as well as with passive detectors (CR-39 based), with modest to good signal-to-noise ratio.

Table 2. LENR experiments with reported charged particle spectra.

Author	Year	Ref.	MeD	Type	Detector	Energies (MeV)	Particle(s), if identified
Taniguchi	1989	[50]	PdD	electrolysis	SSB	< 3	
Aiello	1990	[51]	PdD	gas loaded	SSB	1.8	^{1}H
Cecil	1990	[52]	PdD	ion beam, current	SSB	3,5	^{1}H, ?
Chambers	1990	[11]	PdD	ion beam	SSB	21	^{3}He or ^{4}He ?
Chambers	1991	[12]	TiD	ion beam	SSB	$\sim$5	^{3}H ?
Chambers	1991	[13]	TiD	ion beam	SSB	5-6	^{3}H ?
Cecil	1991	[53]	TiD	gas loaded, current	SSB	1-10	^{3}He, ^{4}He ?
Taniguchi	1991	[54]	PdD	electrolysis	SSB	< 3	
Mo	1991	[55]	TiD,PdD	gas loaded	SSB	> 5	
Tsarev	1991	[56]	TiD,PdD	ion beam	SSB	< 4	^{1}H,^{3}H,^{3}He
Karabut	1992	[57]	PdD	glow discharge	SSB	< 20	^{4}He
Yamaguchi	1993	[58]	PdD	gas loaded	SSB	3-6	^{1}H, ^{4}He
Taniguchi	1994	[59]	PdD	electrolysis	SSB	< 10	
Karabut	1995	[60]	PdD	glow discharge	SSB	≥ 10	$\geq$ ^{4}He
Lipson	2000	[40]	PdD	electrolysis	SSB, CR-39	1-3	^{1}H, ^{3}H
Lipson	2002	[61]	PdD	electrolysis	CR-39	≤ 22	^{1}H, ^{4}He
Lipson	2003	[62]	PdD	electrolysis	SSB, CR-39	1-3	^{1}H, ^{3}H
Jones	2003	[49]	TiD	gas loading	plastic, glass	2.6	^{1}H
Roussetski	2004	[63]	PdD	electrolysis	CR-39	< 10	^{4}He
Lipson	2005	[64]	PdD	electrolysis	CR-39	≤ 16	^{1}H,^{4}He
Kitamura	2011	[65]	PdD	gas loading	SSB	2-8	
Mosier-Boss	2014	[66]	PdD	electrolysis	CR-39	≤ 20	^{1}H, ^{4}He
Lukosi	2014	[67]	PdD	gas loading	diamond	< 14	
Weaver	2015	[68]	PdD	gas loading	diamond	< 8	
Zhou	2015	[69]	PdD	electrolysis	CR-39	< 15	^{1}H, ^{4}He
Ziehm	2022	[70]	PdD	glow discharge	CR-39	0.14	^{4}He

To some observers it was apparent early on that there was more to the spectrum than could be accounted for by dd-fusion reactions (see the prescient comment at the end of Ref. [50]). Particle identification with silicon surface barrier (SSB) detectors with dE-E detection is reported in Ref. [62], and illustrated in Figure 1. Alpha particles are identified with energies between about 9 MeV and 12 MeV. This is consistent with many of the observations of energetic alphas reported in Table 2. In some experiments, a small number of very energetic charged ions are reported; as in Ref. [11] (21 MeV); Ref. [57] (18 MeV); and Ref. [66] (10-20 MeV).

2.3. Discussion of Prior Experiments and Associated Challenges

In general, the reported levels of energetic nuclear particles are not commensurate with reported levels of excess heat production, or with reported tritium production, which historically has hindered understanding of what nuclear processes may be involved and which has limited the usefulness of standard nuclear diagnostics in such experiments. Early on in LENR research, there were claims of observed neutron emission, which provided motivation to carry out measurements aimed at dd-fusion products. However, while at times observing such products, the deployment of nuclear diagnostics for such measurements has also suggested that neutrons and energetic ions are present at energies that are not commensurate with conventional dd-fusion reactions.

In the neutron spectra reported in the papers listed above, 2.45 MeV neutrons that correspond to dd-fusion are detected near the expected energy. Note that neutrons interact weakly with the experimental environment prior to detection, therefore the recorded neutron energy can be expected to be near the neutron energy at their origin. Energetic charged ions, in turn, interact with the experimental environment more strongly, losing energy as they traverse the

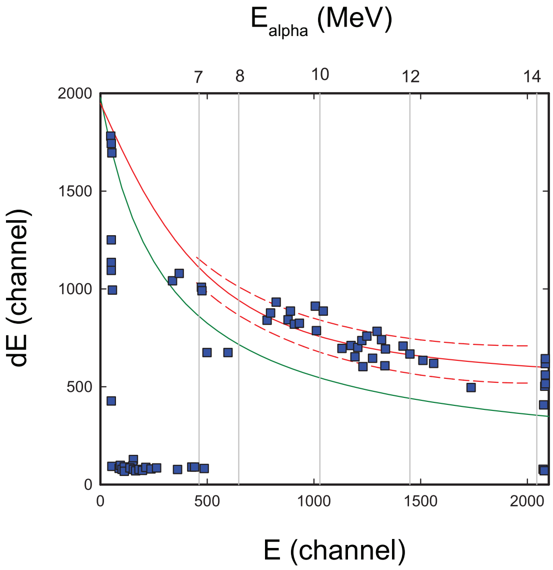

Figure 1. Data redrawn from Lipson et al (2003): blue squares; alphas fall within the red dotted lines around the solid red line; protons fall around the green line; alpha energies are indicated by the grey vertical lines.

sample. Protons from dd-fusion are born with 3.02 MeV and could show up in detectors around 2.6 MeV in [49] due to this energy loss. At present, we do not know with certainty what nuclear processes may lead to alpha emission in LENR experiments at precisely what energies. The degradation of alpha energy in the sample further complicates the situation.

The above issues point at the need for further experiments, where some of these challenges are addressed. This has been the goal of the experiments reported on below.

3. Equipment and Samples in Our Experimental Campaigns

The vacuum chamber used in the experiments reported here is a spherical chamber 304 SST model SP1800SEP from Lesker, with a primary 400 L/s turbo-molecular pump from Edwards model nExt-400, and a 15 cubic feet per minute scroll pump from Edwards model nDds-15.

The ion gun is model DC-25 from Oxford Applied Research. The ion gun specifications give the beam energy as 100-1000 eV, a beam current up to 40 mA (the collected current on target is less by on the order of 10x per our measurements) and a beam diameter of 25 mm.

The deuterium gas used is 99.8% pure from Sigma-Aldrich product number 361860. The Ar gas used is ultra high purity grade 5.0 from Airgas.

A schematic of the ion gun, vacuum chamber, sample, and charged particle detectors is shown in Figure 2. A photograph of the basic system in 2019 is shown in Figure 3.

Since we were interested in the detection of energetic alpha particles (such as the 21 MeV He ions from PdD reported by Chambers [11], the energetic alphas near 20 MeV reported by Karabut [57], and also by Lipson [61]), thick silicon surface barrier (SSB) detectors were used. We worked with two Ortec/Ametek charged particle detectors: one

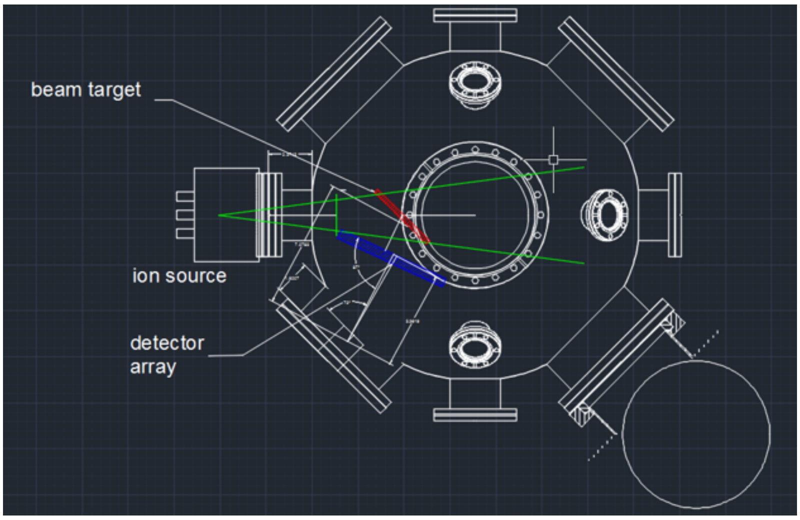

Figure 2. Experimental setup for the 2019 experiments. The ion beam cone is shown in green, the target in red, and the detector mount in blue.

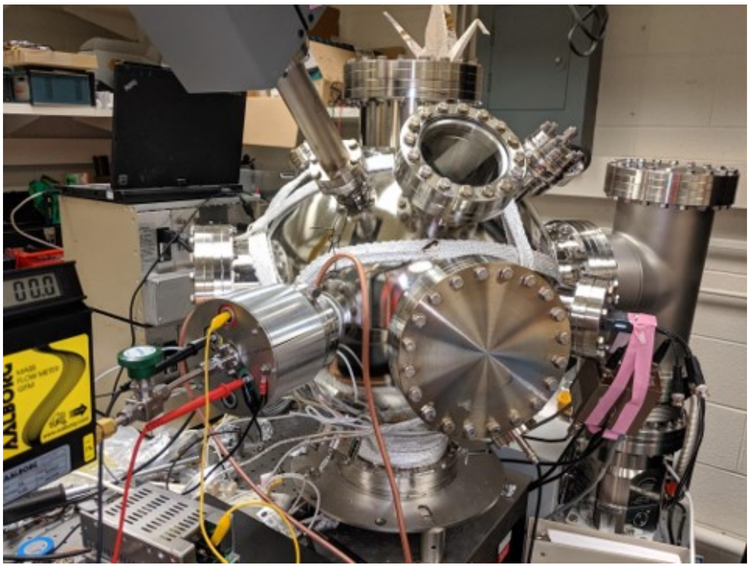

Figure 3. Chamber and ion gun (left front).

is a 500 μm thick ruggedized charged particle detector model number BR-015-050-500 (R-series) with area 50 mm^2; the other is a 2000 μm thick detector model number BA-017-050-2000 (A-series) also with area 50 mm^2.

The R-series detector was used in the 2019 experiments and its bias voltage is -180 V. The larger A-series detector was used in the 2022 experiments and its bias voltage is +250 V. The detectors were calibrated using an ^{241}Am source, with the 5.486 MeV peak in vacuum centered on channel 1730 (out of 16000 channels), following the procedure outlined in Experiment 4.1 of the documentation on the Ortec/Ametek website [71]. A calibration spectrum obtained in 1 atm He at 2 mm distance is shown in Figure 4. For reference, the expected range of energetic alphas and protons at normal incidence in silicon is shown in Figure 5 (based on the SRIM code [108]).

We used a Wendi-2 neutron detector from Thermo Fisher Scientific (formerly Thermo Eberline) model FHT 762 with a 2 bar ^{3}He counter tube and FHT 642 P preamplifier.

For the 2019 experiments, we used a 1.59 mm thick Ti foil with area 50 mm $\times$ 100 mm made of commercially pure (grade 2, ASTM B625) Ti from McMaster-Carr. For the 2022 experiments, we used 0.005 mm thin Ti foils with area 25 $\times$ 25 mm and with purity 99.6+% from Millipore/Sigma (part number GF16653696).

4. Experimental Protocols

The topic of experimental protocols is critical to LENR experiments in general, and to the ion beam experiments discussed below in particular. At issue are the questions of exactly what conditions are sought in an experiment, and why. Much of the discussion about LENR experiments in previous years has avoided focusing on what features of an experiment are deliberately sought and for what reasons. In our experimental campaigns, the employed conditions were motivated by a concrete theoretical picture, which will be briefly reviewed below (and has been discussed in more detail elsewhere [72], [84], [101]).

Historically, there has been no generally agreed upon theoretical model for LENR anomalies, so this discussion of protocol reflects our viewpoint on the hows and whys under consideration. In the model we have advanced, excitation is transferred from D_2/^{4}He transitions to nuclear molecule states in host lattice nuclei, as described in [72]. We then need molecular D_2 species in intimate contact with an acoustic (preferably compressional) lattice vibrational mode. Although deuterons are relatively close in molecular D_2 in gas (on the order of 74 pm), there is no coupling in a gas to other nuclei via shared vibrational modes that exist in a solid.

Molecular D_2 can exist as molecules in some insulators, but the thought is that significant screening occurs in metals, which motivates how to get D_2 molecule-like species to form inside a metal. The basic problem is that in bulk metals in general the background electron density is sufficiently high that anti-bonding orbitals become occupied, pushing the deuterons further apart [73]–[75]. This directs attention to the lower electron density regions that can occur near host lattice metal atom vacancies and in other defects [76], [77].

Palladium stands out from other metals in that a single atom can bind with molecular H_2 or D_2 to form a dihydrogen or dideuterium complex. In such a complex, the metal atom binds to the (spherical) hydrogen or deuterium molecule, and not to the individual atoms of the molecule [78]–[80]. The ground state of the PdD_2 molecule is palladium dideuterium. Metal dideuterium states are low lying (but not the ground state) for other noble metal atoms [81]–[83]. The conjecture is that deuterium atoms in monovacancies in PdD_x spend some of their time in dideuterium complexes near Pd atoms of the lattice [84], where screening may be enhanced, and where substantial coupling to vibrational modes can occur. A similar picture applies to D_2 and HD in monovacancies in nickel deuteride and in a mixed deuteride/hydride. The supposition here is that a similar picture also applies to monovacancies in TiD_x.

The vacancy formation energy in Pd is over 1.5 eV [85], [86] which means that there are few vacancies in thermal equilibrium near room temperature. Hydrogen isotopes in Pd and in Ni generally occupy octahedral sites (O-sites) in bulk material [87], where the background electron density is substantial, and where the binding is not as strong as in a trap (with lower background electron density) [88], [89]. This means that if a Pd atom is removed in PdH_x, the H atoms become trapped (and hence more strongly bound), which lowers the vacancy formation energy of the Pd vacancy. At high H/Pd loading, vacancy formation becomes more probable over a wide range of temperatures (including room temperature), so that in time spontaneous vacancy formation is surmised to lead to a high vacancy concentration (up to 25%, depending on how highly loaded) [90]. Vacancy diffusion from the surface is slow near

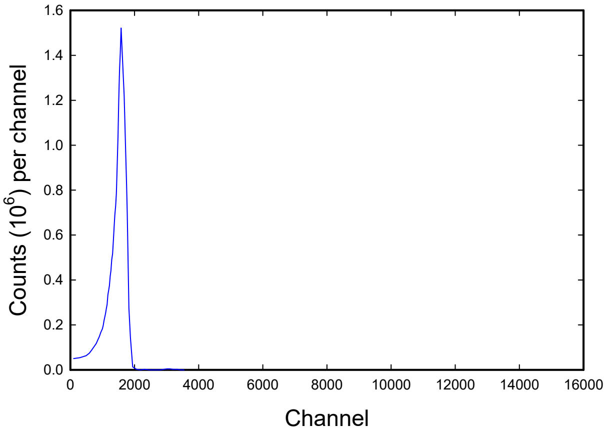

Figure 4. Calibration spectrum in 1 atm helium from ^{241}Am calibration source. The counts at the peak correspond to alphas with energies of about 5.5 MeV.

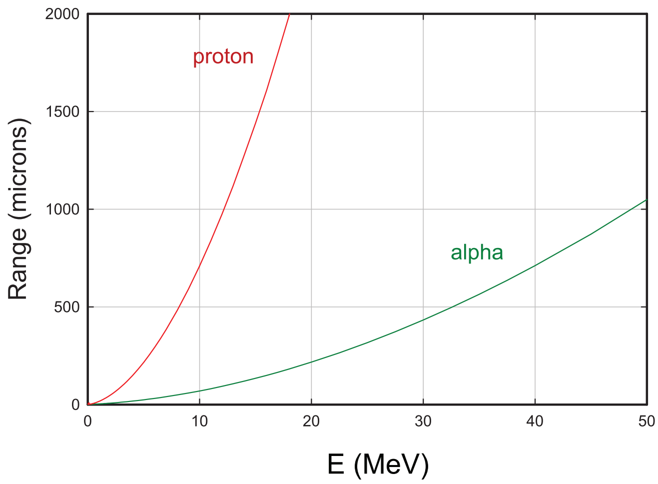

Figure 5. Alpha (dark green) and proton (red) range in silicon as a function of ion energy, based on the SRIM code [108].

room temperature, so some stimulation (such as elevated temperature) can facilitate massive vacancy formation on short (hour) time scales [91], [92]. The argument is that, when the D/Pd ratio is high in a LENR experiment, vacancy formation is favored thermodynamically, and that in some experiments, there are mechanisms available to greatly speed up vacancy formation such that di-deuterium complexes can form in the resulting low background electron density regions. In the 1990s, Szpak and coworkers reported the rapid onset of excess heat in a PdD co-deposition experiment [93]. We had conjectured that in this experiment Pd co-deposition at high current density resulted in a high D/Pd ratio near the surface, which resulted in substantial vacancy formation, since newly formed PdD layers would naturally tend toward the thermodynamically favored configuration [94]. The good reproducibility of excess heat with the subsequently developed Letts co-deposition protocol supports this notion [95], [96]. Low-level energetic charged particle and neutron emission is observed in Pd co-deposition experiments with the related SPAWAR protocol [97]–[99]. The conjecture here is that the current density is lower in this co-deposition configuration, resulting in fewer vacancies so that the coherent dynamics contemplated in [72] are incomplete and low-level nuclear emissions occur instead of excess heat.

The background electron density in Ti is lower compared to Pd so that H and D are more strongly bound, which raises the question to what extent the same conjectures apply. Transferring the intuition about Pd to Ti suggests that what is needed to create sample conditions of interest is the use of deuterium implantation with the ion beam to develop high D/Ti loading, and then the use of D or Ar bombardment to create vacancies near the surface. The same high loading is then expected to result in occupation of the vacancies and formation of dideuterium complexes in contact with Ti atoms at the surfaces of monovacancies.

There has been much discussion of triggering of LENR experiments over the years. In the case of excess heat, in experiments of the early years following the 1989 Fleischmann-Pons announcement, a palladium cathode with high loading might sit and not exhibit any effects for extended periods of time, or might produce excess heat spontaneously. In experiments at SRI, it had been noted that a current ramp could "trigger" excess heat [100], which was thought to be connected with optical phonon generation associated with deuterium flux through the PdD_x [101], during which deuterium chemical potential energy may be converted to optical phonon energy (from our point of view, optical phonons were thought to stimulate the coherent nuclear dynamics then as now). Other related approaches to triggering are conceivable [102], including laser stimulation and electrical current stimulation. Our models suggest that strong excitation of acoustic vibrational modes allows for Dicke enhancements and optical phonon model excitation and plasmon excitation allow for energy exchange during coherent transitions; which implies that a combination of triggers is needed.

In the 1990s at SRI International, there was discussion that loading and triggering were separate functions, even though in early experiments, deuterium loading would be accompanied by deuterium flux which was a trigger (loading and trigger were mixed together), and that this could be used to advantage. This notion served as the foundation for the experiments of [103], in which cathodes were initially highly loaded and cooled, and then triggered using an electrical current pulse to heat the cathode and drive a strong deuterium flux for triggering. Yamaguchi and Nishioka worked with a loaded PdD_x sample with a blocking oxide layer that was then heated and outgassed, resulting in the observation of excess heat, neutron emission, and charged particle emission at different times [58], [104], [105]. Similar ideas were explored in the experiments by Lipson and coworkers [40], [62].

With this as preamble, in our ion beam experiments the idea was to initially load with D (and make some vacancies near the surface in the process), and then to make more vacancies and to trigger LENR reactions using Ar ion bombardment. We also considered stimulating vibrations (especially in the optical phonon modes) with the Ar beam; however, the results of our experiments lead us to conclude that triggering by outgassing is likely a bigger effect.

5. Thick TiD_x Samples in 2019 Experiments

In early tests of the system, we carried out exploratory experiments and observed counts on the R-series charged particle detector (the A-series detector was not yet operating during these early experiments), when a Ti foil was used as the ion beam target. Our principal focus at the time was on high-energy charged particles, and in one experiment, a small number of counts near 30 MeV were seen with the 500 μm 50 mm^2 R-series detector. An example is shown in Figure 6.

In this set of experiments, a 1.59 mm thick Ti foil was used, and kept in the chamber for multiple D loading and Ar bombardment cycles. In the experiment of Figure 6, D ions were implanted at 950 eV with a beam current near 0.5 mA for 1.7 hours, then near 0.63 mA for about 2.75 hours. Ar ion bombardment at 950 eV was then used for 0.25

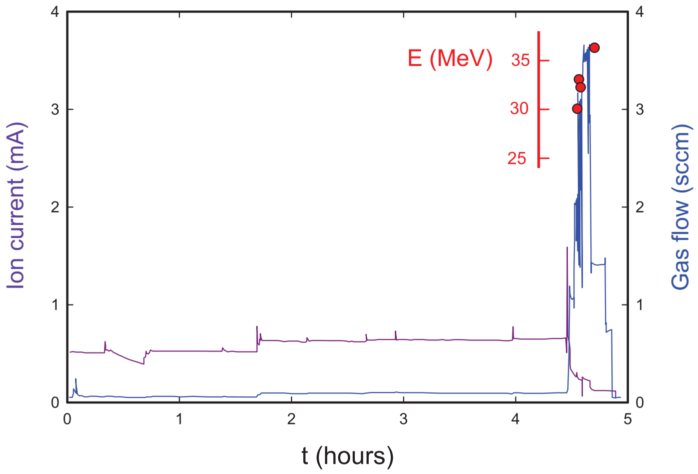

Figure 6. Ion beam current (purple) as a function of time (left y-axis); gas flow (blue) out of the chamber as a function of time (right y-axis); energetic ion counts (red circles) as a function of time (inset y-axis). The ion energies are estimated based on the calibration described in the text.

hours for driving vibrational modes and facilitating defect formation. An initial Ar ion current spike up to 1.5 mA can be seen in the figure (in purple), after which the current on target decreases to below 0.5 mA. Outgassing of the D in the sample is stimulated by the Ar ion bombardment as shown in blue. About 5 minutes after the Ar ion bombardment started, four very energetic charged particles were observed over a period of about 9 minutes on the R-series detector. This detector was located on the front side of the Ti target, 80 mm away from the center of the beam on the sample), so that the detection efficiency is 6.2×10^{-4} (assuming unit detection efficiency for particles that hit the detector).

While the charged particle detectors could not be calibrated at high energy near 30 MeV (due to the absence of radioactive calibration sources with emission in that range), the response of a thick SSB detector is expected to be reasonably linear with particle energy for low-Z charged particles (see Figure 7 and references therein), which suggests that the calibration of the detector at low energy has benefit in connection with high energy particles. We can be certain that the energy of such particles is high (more than 25 MeV), but it is difficult without dedicated calibration in this energy regime to be precise.

The particles cannot be protons (or deuterons or tritons) since their stopping range near 30 MeV is much larger than the R-series detector thickness (500 μm). The range of a 32.5 MeV alpha at normal incidence in silicon according to the SRIM code is 500 μm. At higher energies, alphas pass through the detector with incomplete energy deposition. Monte-Carlo calculations done with the SRIM code indicate that the energy deposited decreases at higher energies, as shown in Figure 8. It is possible that the use of a low-energy calibration leads to an over-estimate in the high-energy range on the order of 15%, resulting in an estimate near 37 MeV in a detector incapable of registering more than 32.5 MeV for alphas at near normal incidence, assuming that the observed counts originate from alpha particles.

A burst of counts on the Wendi-2 neutron detector was recorded starting just before the first energetic charged particle was registered, as shown in Figure 9. We plan to discuss the obtained neutron data in more detail in further reports and will focus here on data from the charged particle detectors.

Next, we report a run carried out two days later, in which a count was observed in a high-energy channel also during the Ar ion bombardment following loading via D bombardment (see Figure 10). The protocol used was similar (with less D implantation since the sample still had D from previous loading cycles without breaking vacuum) and this time, a single very energetic charged particle was observed during the Ar bombardment.

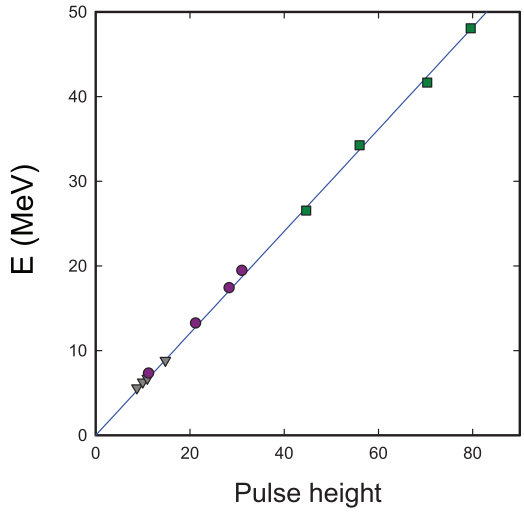

Figure 7. Calibration data of Elliott (1961) for a 3.38 mm lithium drifted silicon detector. Data for Th-228 alphas (grey triangles); data for energetic deuterons (purple circles); data for energetic alphas (dark green squares); linear calibration (blue line).

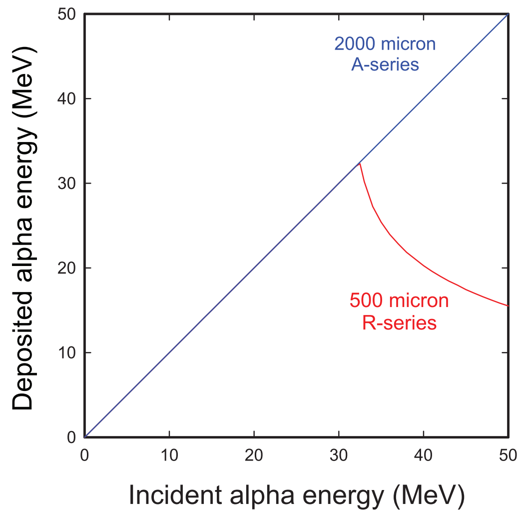

Figure 8. Results of SRIM calculations for incomplete energy deposition for alphas at normal incidence on a 500 μm thick silicon detector (red), relevant for the R-series detector; and for complete energy deposition (blue), relevant for the A-series detector.

6. Thin TiD_x Samples in 2022 Experiments

Following a prolonged interruption due to the pandemic, and also due to using the apparatus for experiments with H on Li targets, we returned to experiments with D on Ti targets in 2022. For these runs, the experimental setup was

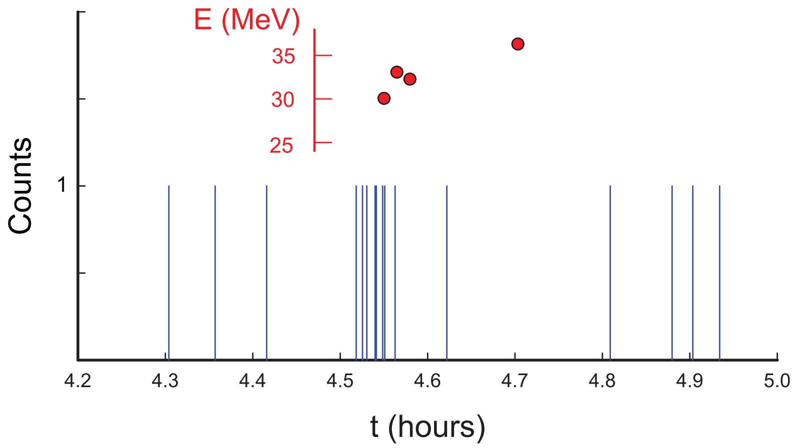

Figure 9. Neutron counts (blue) correlated in time with charged particle counts (red).

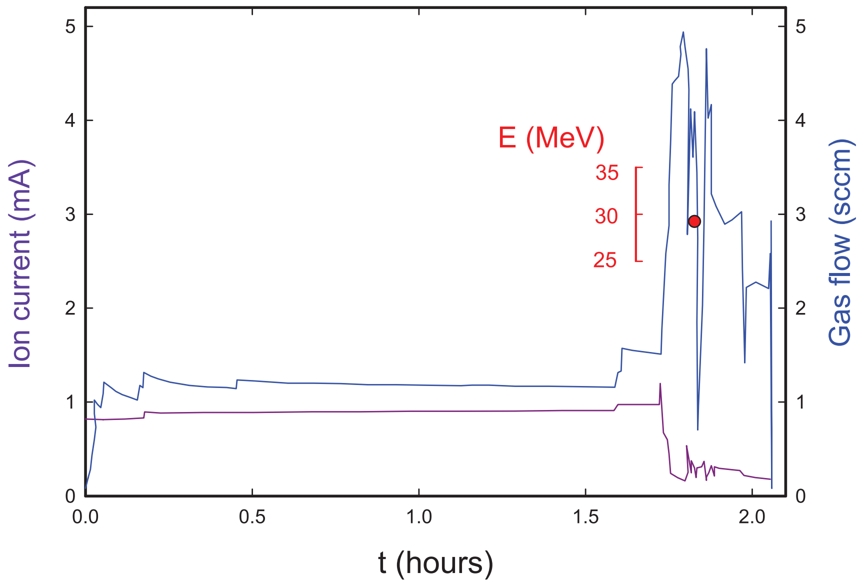

Figure 10. Ion beam current (purple); gas flow (blue) out of the chamber as a function of time; and an energetic ion count (red circle); all similar to what is shown in Figure 6.

reconfigured and the 50 mm^2 A-series detector (2000 μm thick) was positioned close behind the Ti foil, as illustrated in Figure 11. This was done to increase the solid angle relative to the 2019 configuration, where the charged particle detectors were mounted further away. However, upon implementing this change, we recognized that it also affected the experiment in unforeseen ways. The use of thinner Ti foils reduces outgassing, which had become sufficiently small

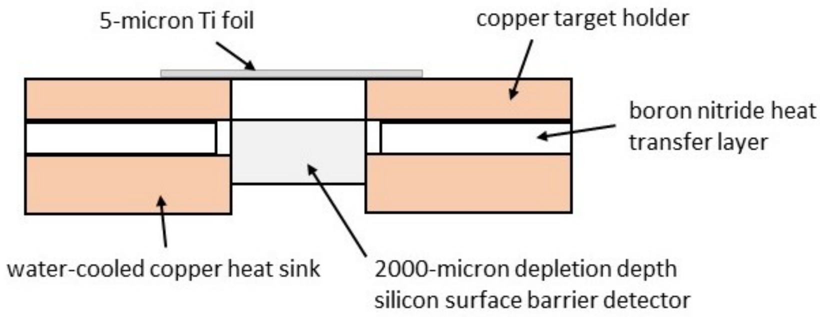

Figure 11. Sample holder, charged particle detector (both in rotational symmetry) and sample cross section (not exactly to scale). For reference, the Ti foil dimensions are 25 mm $\times$ 25 mm and the detector area is 50 mm^2.

to be unmeasurable in the 2022 experiments. There was in addition some degradation of the ion gun during the H-Li experiments, which limited the deuterium beam current compared to the 2019 experiments. As a result, with the new large-solid-angle detector configuration, we have yet to achieve again experimental conditions comparable to the 2019 experiments.

Energetic particles in the 5-6 MeV range of the spectrum from TiD samples are assumed to be alpha particles in the discussion that follows in this section. According to the SRIM code [108], 6 MeV alpha particles have a range of 20 μm in Ti, which motivated us to work with a thin 5 μm Ti (free-standing) foil in these experiments.

Results from one experiment are shown in Figure 12, where counts from the thick 2000 μm A-series detector behind the sample are shown as a function of time, with a short time window on the left focusing on the Ar bombardment, and a much longer time window on the right focusing on the absence of counts at later times in this experiment. Following previous experiments, where the sample was loaded with deuterium, in this experiment the sample was loaded with deuterium for two hours at 0.20 mA beam current and 950 eV beam energy (the last part of the D implantation is indicated in the figure). Then the Ar beam was run at up to 1.5 mA and at 950 eV for 10 minutes, then turned off.

Note that by design SSB charged particle detectors record noise in the lowermost channels. The cut-off channel for such noise can vary, depending on the experimental configuration. In particular, a temperature increase of the detector predictably leads to a higher noise cut-off channel. Although the sample and detector are water-cooled in this configuration, the detector temperature increases when the Ar beam is on, which moves the low-energy noise to higher channels and raises the noise cut-off channel (as can be seen in Figure 12). The high cut-off corresponds to a charged particle energy near 1 MeV, and the lower cut-off corresponds to about 0.36 MeV.

Also note that throughout these experiments, no counts have been registered in the channels above the noise cut-off channel, except for the counts reported in the figures. The absence of high-energy counts across prolonged periods of time (e.g., across about 25 hours in Figure 12) leads to the conclusion that the background of high-energy charged particles is very low.

We do not have particle identifications for these counts in our experiment. An estimate for the energy loss

$$\delta E = \frac{dE}{dx}\delta x \tag{1}$$

from the SRIM code [108] for an alpha going through 5 μm of Ti (at normal incidence) is shown in Figure 13. This suggests that if an alpha was born near the front surface, it would lose at least 1 MeV traversing the Ti foil. In Figure 14, the average energy of a 6.6 MeV alpha that traverses a 5 μm Ti foil is shown as a function of angle. These considerations provide a first estimate of the initial alpha energy within this scenario, but we would need a spectrum

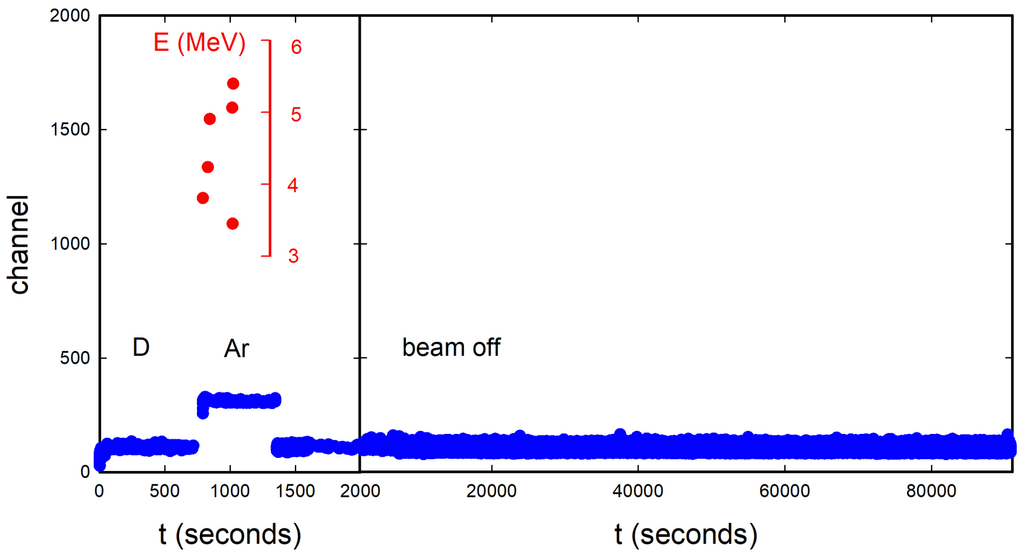

Figure 12. Counts as a function of channel from the A-series detector (Experiment 5j). The uppermost channels with low-channel noise are shown in blue; charged particle counts are shown in red. Corresponding particle energies are indicated by the inset axis in red. Note that different time scales are used for the 33 minutes around the time of the Ar bombardment (in the part of the figure on the left) and for the more than 25 hours of data taken after the Ar bombardment (in the part of the figure on the right).

from both sides of the sample in the same experiment, along with particle identification, to be certain of the precise particle energies.

Data from a later loading/bombardment cycle on the same sample (done in the same experimental configuration and on the same sample without breaking vacuum) is shown in Figure 15. In this case, a single energetic count appears near the end of the 10-minute Ar bombardment, after which counts are recorded that correspond to particle energies up to 11 MeV in a 42-hour-long burst event. Of interest is that these later counts were measured when the ion beam was already off. This further supports the notion that there is no possibility of interference with detector operation in the high-energy range due to the ion beam.

Analogous to the R-series detector of the 2019 experiments, the A-series detector was not directly calibrated above 30 MeV, so the extrapolated energies are estimated based on the low-energy calibration done with ^{241}Am. Six very energetic particle counts are seen above 37.5 MeV (estimated based on the low-energy calibration) across five different experiments in the 2022 experimental campaign. Based on these observations, and taking into account the earlier front-side measurements with the R-series detector in 2019, we expect these counts to correspond to alpha particles in the 32-40 MeV range.

7. Nuclear Reactions Directly Associated with the Ar Beam

Incoming Ar ions at 950 eV would not be expected to result in nuclear reactions based on binary collisions, due to the large associated Coulomb barriers. Fusion reactions between ^{40}Ar and ^{48}Ti have been observed in Ref. [109] with Ar ions at 325 MeV. Fusion excitation cross sections in the lab frame for the closely related ^{40}Ca+^{40}Ca reaction are given in Ref. [110] near threshold in the vicinity of 100 MeV.

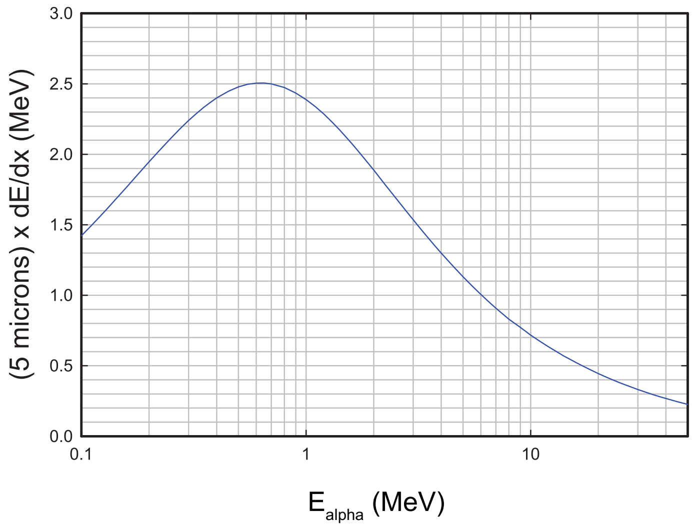

Figure 13. Energy loss for an alpha particle normal through 5 μm of Ti as a function of energy.

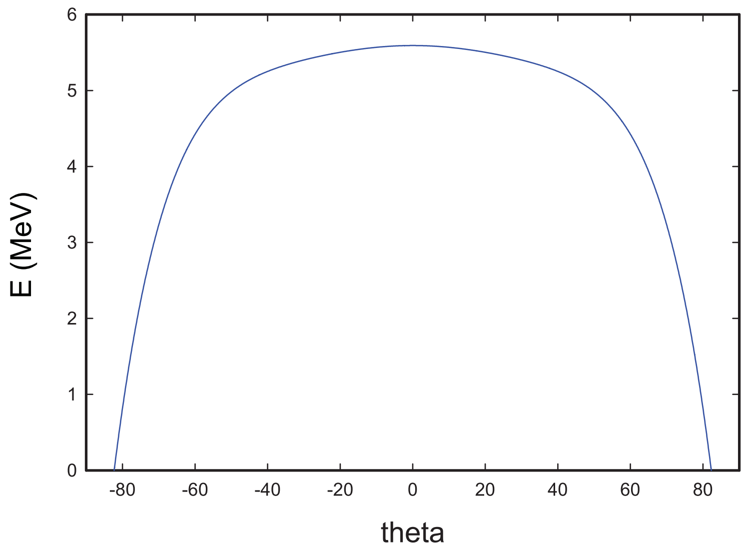

Figure 14. Energy of a 6.6 MeV alpha particle passing through 5 μm of Ti as a function of angle.

Ar ions could in principle interact with deuterons to cause nuclear reactions. Such reactions were studied in Ref. [111]. Of interest might be cross sections for the (d,p) and (d,α) reactions. According to the ENDF nuclear data library [112], the cross sections for these processes are at the μ-barn level at 1 MeV relative energy, and

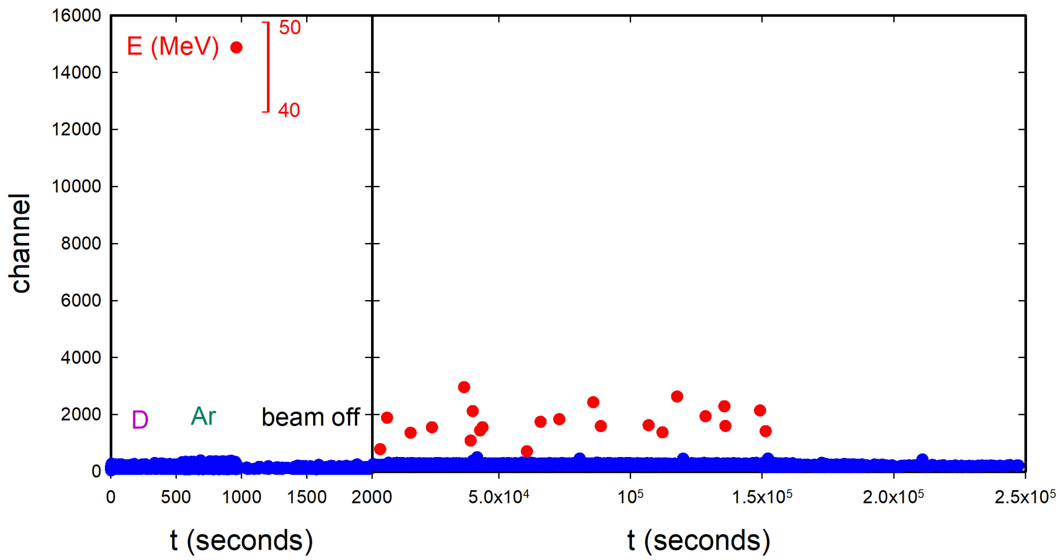

Figure 15. Counts as a function of channel from the A-series detector (Experiment 5k). The uppermost channel for the low-channel noise is shown in blue; charged particle counts shown in red. Corresponding particle energies indicated by the inset axis in red.

fall exponentially to lower values as the relative energy decreases. Based on such considerations, no reactions are conventionally expected with incident Ar ions at 950 eV.

It could be argued that incoming Ar ions could transfer energy directly to deuterons through collisions. It is possible to estimate the maximum D energy in an elastic collision leading to:

$$E_d = \frac{4M_d M_{Ar}}{(M_d + M_{Ar})^2} E_{Ar} \tag{2}$$

where E_{Ar} is the energy of the incident Ar ion, and where E_d is the maximum outgoing deuteron energy possible. In the case of a 950 eV ^{40}Ar ion, this evaluates to:

$$E_d = 0.18 \cdot E_{Ar} = 172 \text{ eV} \tag{3}$$

The deuteron-deuteron fusion cross section for a 172 eV deuteron on a deuteron at rest is negligible, even with the strong screening seen in low-energy deuteron beam experiments [5]–[10]. Hence, no knock-on dd-fusion reactions would be expected from the Ar bombardment.

8. Discussion

Low-level MeV ion emission from metal deuterides has been reported previously [11]–[13], [49]–[70]. In experiments with TiD_x, deuterium loading was done using gas loading [52], [49] or an ion beam [12], [13], [56]. Triggering of the charge emission was in our view likely achieved either by outgassing [12], [13], [56], [49] or by driving with an electrical current [52]. In the experiments reported on in this paper, the Ti foils were loaded by ion beam implantation, and we surmise that D outgassing provides the trigger, when the Ar ion beam is on (with much more outgassing occurring with thicker samples than with thinner samples). It may be that outgassing is also responsible for triggering low-level charged particle emission after the Ar ion bombardment, while it is also possible that mechanical relaxation acts as a trigger.

While dd-fusion products were reported in the Jones experiment [49], evidence for higher energy particles from TiD_x is claimed in the experiments of Chambers [12], [13] and Cecil [53]. Our results so far support the notion of particles not emitted due to conventional dd-fusion reactions. Based on reported data from these previous experiments, the observed counts there likely correspond to low-mass ions (perhaps tritons in [13], and protons through alpha particles in [53]). While we have also reported on detector counts that correspond to particle energies below 11 MeV, our experimental configuration does not allow for particle identification in this energy range.

Energetic ion emission at very high energy (near 20 MeV) has been claimed with PdD_x samples [11], [57], [66], which motivated our experiments. PdD_x has been studied more than TiD_x, and there are few reports of very energetic particles in this range from TiD_x (one exception are some CR-39 counts at very high energy on one slide from Lipson's ICCF13 talk at Sochi in 2007). We are not aware of earlier claims of low-level energetic charged particles in the 32-40 MeV range from TiD_x. This is a new (and preliminary) result of our experiments presented in this paper.

High multiplicity events in the case of low-level neutron emission were often discussed in the early days of LENR research (such as in [113]), which suggests that they might occur also in charged particle emission (as reported in [54]). We reported on data that suggest the occurrence of a high multiplicity neutron emission event, although we will need to continue to monitor for such potential effects in future experiments with upgraded neutron detection configurations.

An important question is: what should be done next to improve the experiment and results to date? We consider the detector counts that correspond to very energetic particles in the 32-40 MeV range as the most important lead, since such purported signals can provide valuable information about mechanisms at play (as further discussed below). So future research should emphasize clarification of this issue in our view.

A major goal is the increase of the conjectured energetic charged particle emission flux. If low-level charged particle emission is triggered by outgassing in these experiments (which is consistent with the larger count rate seen from thicker Ti foils), then we would like to increase the thickness of the Ti foils used. Since deuterium diffusion in TiD_x is slow and increases with temperature [114], we then expect a higher count rate if external heating were provided during and/or after the Ar bombardment.

The observable particle count rate could also be increased if we increased the solid angle of the charged particle detector by using a larger area detector. To this end, we are procuring a 450 mm^2 2000 μm thick A-series detector. Arranging for dedicated detector calibration in the high-energy range of 40 MeV and higher has been challenging. Recently we became aware of a cyclotron available at the Crocker Nuclear Lab associated with UC Davis that operates in this regime and that can be used for detector calibration.

The very energetic 32-40 MeV charged particle counts have been observed in our experiments with two different detectors so far (the R-series and the A-series detectors). However, detecting them with a CR-39 detector would add further confidence. For this, it would be important to establish a calibration with alphas at high energy on CR-39; ideally this could be done at the same time as calibrating the SSB detectors.

Particle identification of these very energetic particles could be conducted using dE-E detection. A "thin" dE detector in this case could be a 100 μm thick SSB detector, which would provide for a substantial dE measurement. Particle identification could also be made using a foil to degrade the particle energy. Thicker titanium foils would be useful for increasing outgassing, and could make a minor contribution to energy loss, as shown in Figure 16. Given the low rate of diffusion for deuterium in TiD_x, there is little motivation to go to samples thicker than 100 μm unless the sample is heated to well above room temperature.

Observed energetic particle counts in the 1-11 MeV energy range are also of interest, but requires a different strategy to be pursued. What is of interest ultimately in this regard is the determination of the charged particle identity and particle energy when created, which prompts us to work with thin foils to minimize energy loss through the foil. As discussed above, we saw some counts in this energy range with a 5 μm thick Ti foil, which results in energy loss on

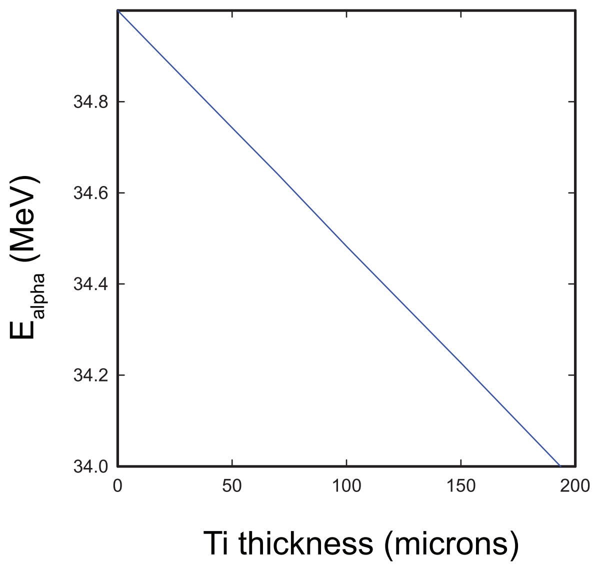

Figure 16. Energy of a 35 MeV alpha after transit at normal incidence through Ti foils of different thicknesses.

the order of 1 MeV for a 6 MeV alpha at normal incidence, less at higher particle energy, and more at lower particle energy (see Figure 13). However, from our experience so far, the thinner foils gave fewer counts of interest. Ideally, a way might be found to work with thinner foils while arranging for enough counts from which a useful spectrum can be acquired. The count rate could be increased with a large area SSB detector placed close behind the foil. Based on the early observations of Cecil [53], we expect that different low-mass charged ions contribute to the spectrum. Consequently, dE-E charged particle spectroscopy would be ideal to achieve further clarification. A large area dE-E detector could in principle be placed close behind a thin foil sample. However, this would allow for charged particles to enter the detector at arbitrary angles, making particle identification much more difficult. Moving the dE-E detector back away from the foil improves the ability to identify particles, but reduces the particle count.

As seems clear from this discussion, different tradeoffs need to be considered in preparation for the next phase of this research. If we accept these limitations, then under consideration is an experiment in which a small area dE-E detector well away from the sample captures counts from a sample emitting at low count rate, which implies the need for long runs so as to build up good statistics. On the other hand, if it were possible to arrange for a μm-scale Ti surface layer (with lots of vacancies) on a thick Pd deuterium reservoir (with no vacancies), then it may be possible to arrange for a substantial sustained D flux moving through the Ti sample, with the goal of causing sustained charged particle emission at a comparatively high level, so that a small-area dE-E detector well away from the front surface could accumulate a useful spectrum in a reasonable amount of time. The latter setup requires mindfulness about the possibility of induced charged particle emission from the PdD substrate, which could confound the TiD results. Another possibility is to attempt triggering with an electrical current through a loaded TiD_x thin film.

Also of interest is the implementation of a version of the experiment with PdD_x and other metal deuterides. One aspect that is peculiar to TiD_x is the low diffusion coefficient. This suggests that working with PdD_x at low temperature initially is appropriate, and that triggering with an even higher D flux would be possible during heating with the Ar ion bombardment.

Another conceivable improvement is the use of a more efficient neutron detector and the use of shielding for the neutron detector to improve signal-to-noise ratio. This is planned for future work.

Finally, the central question concerns mechanisms that predict and can explain low-level energetic particles emitted from TiD under the given conditions. A brief consideration of theory and candidate particles and energies is given in the Appendix.

Appendix: Energetic Charged Particle Candidates

Historically, there has been no generally accepted theory for LENR anomalies, and most attention has been focused on energetic dd-fusion products and possible rate enhancement mechanisms that may explain them. We have over many years developed comprehensive theoretical models for reported anomalies, which are based on known collective quantum effects such as Dicke enhancement applied to systems of coupled nuclei. Here we provide a brief overview of energetic charged particle candidates that can be expected from these models as candidates to account for the observations. The basic approach is outlined in Ref. [72].

Sufficiently stable nuclear molecule states in Ti

At the core of this picture is the nonradiative transfer of excitation energy from deuteron pairs to resonant or near-resonant excited states of nearby metal nuclei. The coherent nuclear dynamics involved require a great many reasonably stable nuclear excited states, for sequential excitation transfer processes starting from $D_2/^4He$ transitions near 23.86 MeV. In canonical nuclear databases, there are no known stable excited states listed near 23.86 MeV, which has long hindered the development of this kind of model. Recently, we proposed to consider long-lived cluster-based nuclear molecule states as candidate receiver states for the kind of nuclear excitation transfer under consideration. A growing literature exists on nuclear cluster states and some molecule-like formations promise to be particularly long-lived. We considered liquid drop model calculations for cluster-based nuclear states consistent with fission barrier calculations, but had to conclude that the states described by such models are very unstable in the mass and charge regime of interest.

However, calculations in the literature for $^{12}C+^{12}C$ and $^{16}O+^{16}O$ nuclear states show a potential minimum for daughter nuclei that are separated, which suggests that a kind of nuclear molecule is possible where the daughters act as separated clusters (in contrast to highly deformed states in liquid drop model calculations where the clusters nevertheless remain connected). We developed a simple model to estimate the energy for ground state nonrotational nuclear molecules [72]. Nuclear molecule excitation energies for the stable Ti isotopes, as predicted by this model, are shown in Figure 17 as a function of the decay rate of the corresponding state (which does not include radiative or internal conversion decay processes, the rates for which are yet undetermined). The lower energy nuclear molecules are highly asymmetric involving a low mass and charge daughter. Such states, occupied upon receipt of transferred excitation and subsequent tunneling decay, are candidates for low-level charged particle emission. Above about 30 MeV are a great many nuclear molecule states that can participate in the nuclear dynamics. Note that energy levels can shift in quantum systems that are affected by strong coupling, as can be the case due to collective effects such as Dicke enhancement [72], [84], [101].

Very energetic alphas above 30 MeV

The observation of very energetic alphas above 30 MeV appears consistent with the occupation of very high nuclear molecule states above 30 MeV (note that the nuclear molecule excitation energy is indirectly related with the emitted alpha energy).

According to the coherent nuclear dynamics model, the first step is a transfer of the 23.86 MeV quantum from the $D_2/_4He$ transition to a resonant receiver state. With sufficient accumulation of excited state population, subsequent

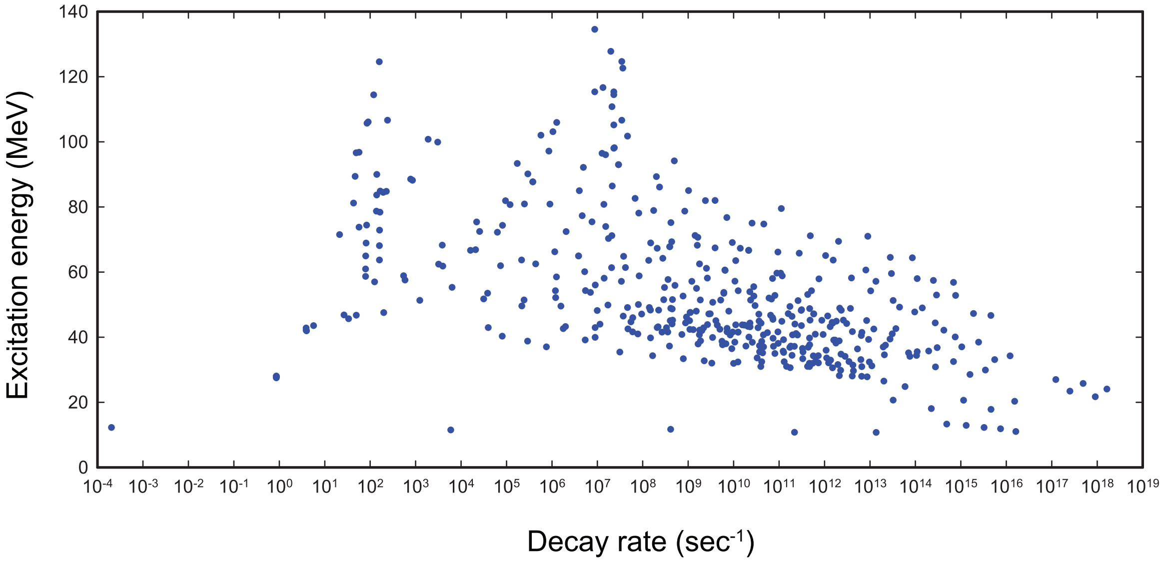

Figure 17. Nuclear molecule state energies as a function of decay rate for the stable Ti isotopes ^{46}Ti, ^{47}Ti, ^{48}Ti, ^{49}Ti, and ^{50}Ti.

third-order transitions occur leading to the accumulation of nuclear molecule population near 47.72 MeV. Depending on the details of the relative nuclear molecule energies, as well as the amount of coherent energy exchange possible with phonons and plasmons, occupation of nuclear molecule states over a range of excitation energies is expected. If the coherent dynamics are frustrated in the sense of not returning the nuclear molecule population back to the Ti isotope ground states, then one would expect energetic decay processes. We have proposed that the decay of these excited states is responsible for reported transmutation effects. Here we note that the ejection of a low-mass fragment (such as an alpha particle) would also be expected as a possible decay path (by analogy with Auger decay in atoms, where an excited electron is ejected interacting with a second electron which is de-excited).

If the energy exchange with vibrations and plasmons is minimal, then the ejected alpha energy depends only on the isotope and excitation transfer from the fusion transition. Candidates to account for the signals in our experiments above 30 MeV include:

$$^{46}\text{Ti} + 2(23.86\text{ MeV}) \longrightarrow (^{Z_b}A_b + {}^{Z_c}A_c) \longrightarrow {}^{42}\text{Ca}(3.45\text{ MeV}) + \alpha(36.2\text{ MeV})$$
$$^{47}\text{Ti} + 2(23.86\text{ MeV}) \longrightarrow (^{Z_b}A_b + {}^{Z_c}A_c) \longrightarrow {}^{43}\text{Ca}(3.30\text{ MeV}) + \alpha(35.4\text{ MeV})$$
$$^{48}\text{Ti} + 2(23.86\text{ MeV}) \longrightarrow (^{Z_b}A_b + {}^{Z_c}A_c) \longrightarrow {}^{44}\text{Ca}(3.19\text{ MeV}) + \alpha(35.1\text{ MeV})$$
$$^{49}\text{Ti} + 2(23.86\text{ MeV}) \longrightarrow (^{Z_b}A_b + {}^{Z_c}A_c) \longrightarrow {}^{45}\text{Ca}(3.06\text{ MeV}) + \alpha(34.5\text{ MeV})$$
$$^{50}\text{Ti} + 2(23.86\text{ MeV}) \longrightarrow (^{Z_b}A_b + {}^{Z_c}A_c) \longrightarrow {}^{46}\text{Ca}(2.96\text{ MeV}) + \alpha(34.0\text{ MeV})$$

Where the notation $(^{Z_b}A_b + {}^{Z_c}A_c)$ is intended to indicate that there are many reasonably stable nuclear molecule intermediate candidates possible. With thick detector calibration between 30 MeV and 40 MeV, particle identification, and with enough counts, it should be possible to either confirm or rule out these candidates in future experiments.

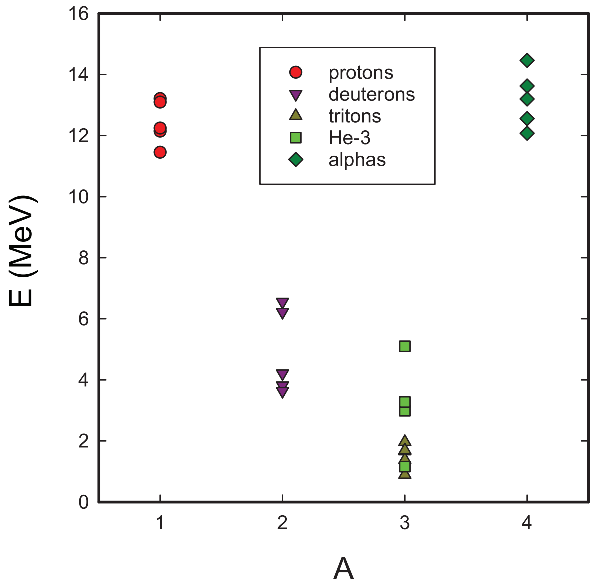

Figure 18. Candidates for low-level energetic particle emission from Ti nuclear molecules near 23.86 MeV.

Low-mass Candidates at Lower Energies

For low-level energetic charged particle emission at lower energy, the same basic approach is proposed, except with only a single fusion quantum exchanged instead of two. If energy exchange with phonons and with plasmons is minimized, then we would expect decay products and energies as illustrated in Figure 18.

In Figure 18, we see that protons and alpha particles are candidates for the higher energy counts, and deuterons, tritons and ^{3}He ions are candidates for the lower energy counts. With a thin foil sample, with a dE-E detector reasonably distant from the foil (so that particle trajectories are near normal incidence), and with a sufficiently high energetic ion emission rate, we expect it to be possible to test for these candidates to be represented in experiments that are weakly driven (to avoid complications due to double excitation and energy exchange).

A highly idealized schematic for the (generalized) excitation transfer processes and nuclear molecule tunnel decays are illustrated in Figure 19. In the nuclear dynamics proposed, the excitation transfer can lead to the occupation of Ti nuclear states near 23.86 MeV and—via up-conversion—states near 2 $\times$ 23.86 MeV, the latter of which are expected to lead to low-level emission of more energetic ions as described above. Excitation transfers among the different nuclear molecule states near 2 $\times$ ΔE allows for coherent energy exchange with vibrations and electrons, which then leads to the possibility of down-conversion to nuclear molecule states in the vicinity of ΔE. The much simplified scheme of Figure 19 is intended to convey the essence of this more complicated picture. Lastly, transfer of excitation back to ^{4}He nuclei can lead to the excitation of unstable ^{4}He states and subsequent decay with the known 3+1 fusion products.

Observability of Nuclear Molecule Energies

Within the model, the nuclear molecule energies are key parameters, which we would like to know accurately. Over the past year we had been optimistic that such information might be gleaned from careful measurements of charged ion

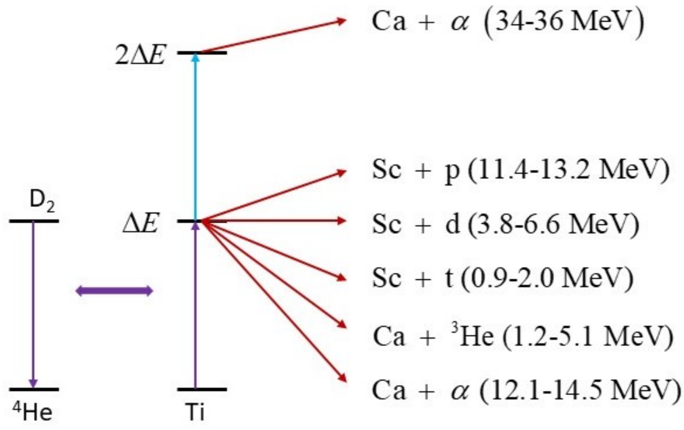

Figure 19. Idealized schematic for excitation transfer to nuclear molecule states and highly asymmetric decay pathways under consideration, where ΔE is the $D_2/^4He$ transition energy of 23.86 MeV. The energies listed are for the low-mass daughters.

energies and particle identifications. However, after some thought, it has become clear that the emitted particle energies are determined by the parent and daughter mass energies, and by the energy transferred from the fusion system, as long as there is not significant energy exchange with plasmons and phonons. The nuclear molecule energy does not come into this calculation.

We have remarked elsewhere [72] that a weak radiative decay of the nuclear molecule states is expected, such that it might be possible to provide further clarification with a very thick NaI gamma detector. Whether or not this would be successful in experiments similar to those described in this paper is not clear at present (since the emission rate is likely small). In any event, we will consider experiments of this sort on different samples in the future.

Acknowledgments

Technical assistance from Jessica Kedziora is much appreciated. Helpful discussion with Igor Jovanovic on the problem of dE-E detection is also much appreciated. Carlotta Barone-MacDonald, Jonah Messinger, and Nicola Galvanetto provided very helpful comments on the manuscript. Financial support (greatly appreciated) for this work came from the Minhas H. Family Fund, and from the Anthropocene Institute.

References

[1] W. Möller, F. Besenbacher and J. Bottiger, "Saturation and isotope mixing during low-temperature implantations of hydrogen into metals," *Applied Physics A* **27** (1982) 19–29.

[2] S. M. Myers, D. M. Follstaedt, J. E. Schirber and P. M. Richards, "Search for cold fusion at D/Pd $>$ 1 using ion implantation," *Journal of Fusion Energy* **9** (1990) 263–268.

[3] S. M. Myers, P. M. Richards, D. M. Follstaedt and J. E. Schirber, "Superstoichiometry, accelerated diffusion, and nuclear reactions in deuterium-implanted palladium," *Physical Review B* **43** (1991) 9503.

[4] G. P. Chambers, J. M. Eridon, and K. S. Grabowski, "Upper limit on cold fusion in thin palladium films," *Physical Review B* **41** (1990) 5388.

[5] F. Raiola, P. Migliardi, L. Gang, C. Bonomo, G. Gyürky, R. Bonetti, C. Broggini, N. E. Christensen, P. Corvisiero, J. Cruz, and A. D'Onofrio, "Electron screening in d(d,p)t for deuterated metals and the periodic table," *Physics Letters B* **547** (2002) 193–199.

[6] F. Raiola, L. Gang, C. Bonomo, G. Gyürky, M Aliotta, H. W. Becker, R. Bonetti, C. Broggini, P. Corvisiero, A. D'Onofrio and Z. Fülöp, "Enhanced electron screening in d(d,p)t for deuterated metals," *The European Physical Journal A – Hadrons and Nuclei* **19** (2004) 283–287.

[7] F. Raiola, B. Burchard, Z Fülöp, G. Gyürky, S. Zeng, J. Cruz, A. Di Leva, B. Limata, M. Fonseca, H. Luis and M. Aliotta, "Electron screening in d(d,p)t for deuterated metals: temperature effects," *Journal of Physics G: Nuclear and Particle Physics* **31** (2005) 1141.

[8] A. Huke, K. Czerski and P. Heide, "Accelerator experiments and theoretical models for the electron screening effect in metallic environments," *Proc. ICCF11* (2006) 194–209.

[9] A. Huke, K. Czerski and P. Heide, "Measurement of the enhanced screening effect of the d+ d reactions in metals," *Nuclear Instruments and Methods in Physics Research Section B: Beam Interactions with Materials and Atoms* **256** (2007) 599–618.

[10] K. Czerski, A. Huke, L. Martin, N. Targosz, D. Blauth, A. Górska, P. Heide and H. Winter, "Measurements of enhanced electron screening in d+d reactions under UHV conditions," *Journal of Physics G: Nuclear and Particle Physics* **35** (2007) 014012.

[11] G. P. Chambers, J. E. Eridon, K. S. Grabowski, B. D. Sartwell and D. B. Chrisey, "Charged particle spectra of palladium thin films during low energy deuterium ion implantation," *J Fusion Energy 9* (1990) 281–285.

[12] G. P. Chambers, G. K. Hubler and K. S. Grabowski, "Search for energetic charged particle reaction products during deuterium charging of metal lattices," *AIP Conference Proceedings*, American Institute of Physics **228** (1991) 383–396.

[13] G. P. Chambers, G. K. Hubler, and K. S. Grabowski, "Evidence for MeV particle emission from Ti charged with low energy deuterium ions," Naval Research Lab Memorandum Report 6927 (1991).

[14] S. Bartalucci, V. I. Vysotskii and M. V. Vysotskyy, "A search for correlated quantum states in nuclear reactions: First exciting results from an experimental test," *J. Condensed Matter Nucl. Sci.* **36** (2022) 130–136.

[15] S A Lipinski and H U Lipinski, "Hydrogen-lithium fusion device, methods and applications," *United States Patent Application Publication* US 2009/0274256 A1 (2009).

[16] S A Lipinski and H U Lipinski, "Hydrogen-lithium fusion device," *WIPO/PCT Patent Application Publication* WO 2014/189799 A9 (2014).

[17] N. S. Lewis, C. A. Barnes, M. J. Heben, A. Kumar, S. R. Lunt, G. E. McManis, G. M. Miskelly, R. M. Penner, M. J. Sailor, P. G. Santangelo and G. A. Shreve, "Searches for low-temperature nuclear fusion of deuterium in palladium," *Nature* **340** (1989) 525–530.

[18] R. B. Campbell and L. J. Perkins, "A study of cold fusion in deuterated titanium subjected to high-current densities," *Fusion Technology* **16** (1989) 383–387.

[19] G. C. Fralick, A. J. Decker and J. W. Blue, "Results of an attempt to measure increased rates of the reaction ^{2}D+^{2}D yields ^{3}He+n in a nonelectrochemical cold fusion experiment," NASA Technical Memorandum 102430 (1989).

[20] K. I. Thomassen, J. F. Holzrichter, F. T. Aldridge, B. Balke, J. Bowers, D. B. Bullen, M. D. Cable, M. Caffee, R. B. Campbell and C. Colmenares, "Lawrence Livermore National Laboratory (LLNL) research on cold fusion," *Lawrence Livermore National Laboratory Report UCID-21809* (1989).

[21] P. B. Price, S. W. Barwick, W. T. Williams and J. D. Porter, "Search for energetic-charged-particle emission from deuterated Ti and Pd foils," *Physical Review Letters* **63** (1989) 1926.

[22] H. S. Bosch, G. A. Wurden, J. Gernhardt, F. Karger and J. Perchermeier, "Electrochemical cold fusion trials at IPP garching," *Journal of Fusion Energy* **9** (1990) 165–186.

[23] D. Albagli, R. Ballinger, V. Cammarata, X. Chen, R. M. Crooks, C. Fiore, M. P. Gaudreau, I. Hwang, C. K. Li, P. Linsay and S. C. Luckhardt, "Measurement and analysis of neutron and gamma-ray emission rates, other fusion products, and power in electrochemical cells having Pd cathodes," *Journal of Fusion Energy* **9** (1990) 133–148.

[24] J. D. Porter, A. A. Shihab-Eldin, H. Bossy, F. J. Echegaray, J. M. Nitschke, S. G. Prussin, J. O. Rasmussen and M. A. Stoyer, "Limits on electromagnetic and particle emission from palladium-D_2O electrolytic cells," *Journal of Fusion Energy* **9** (1990) 319–327.

[25] H. Wiesmann, “Examination of cathodically charged palladium electrodes for excess heat, neutron emission, or tritium production,” *Fusion Technology* **17** (1990) 350–354.

[26] S. L. Rugari, R. H. France, B. J. Lund, S. D. Smolen, Z. Zhao, M. Gai and K. G. Lynn, “Upper limits on emission of neutrons from Ti in pressurized D_2 gas cells: A test of evidence for cold fusion,” *Physical Review C* **43** (1991) 1298.

[27] S. E. Jones, E. P. Palmer, J. B. Czirr, D. L. Decker, G. L. Jensen, J. M. Thorne, S. F. Taylor and J. Rafelski, “Observation of cold nuclear fusion in condensed matter,” *Nature* **338** (1989) 737–740.

[28] A. Bertin, M. Bruschi, M. Capponi, S. De Castro, U. Marconi, C. Moroni, M. Piccinini, N. Semprini-Cesari, A. Trombini, A. Vitale and A. Zoccoli, “Experimental evidence of cold nuclear fusion in a measurement under the Gran Sasso Massif,” *Il Nuovo Cimento A* **101** (1989) 997–1004.

[29] G. Shani, C. Cohen, A.. Grayevsky and A. Brokman, “Evidence for a background neutron enhanced fusion in deuterium absorbed palladium,” *Solid State Communications* **72** (1989) 53–57.

[30] K. L. Wolf, N. J. C. Packham, D. Lawson, J. Shoemaker, F. Cheng and J. C. Wass, “Neutron emission and the tritium content associated with deuterium-loaded palladium and titanium metals,” *Journal of Fusion Energy* **9** (1990) 105–113.

[31] A. Takahashi, T. Takeuchi, T. Iida and M. Watanabe, “Emission of 2.45 MeV and higher energy neutrons from D_2O–Pd cell under biased-pulse electrolysis,” *Journal of Nuclear Science and Technology* **27** (1990) 663–666.

[32] T. Bressani, D. Calvo, A. Feliciello, C. Lamberti, F. Iazzi, B. Minetti, R. Cherubini, A. M. T. Haque and R. A. Ricci, “A study of the neutron emission from Ti loaded with D in gas phase by means of a time-of-flight spectrometer,” *Proc. ICCF2* (1991) 105.

[33] T. Bressani, D. Calvo, A. Feliciello, C. Lamberti, F. Iazzi, B. Minetti, R. Cherubini, A. M. I. Haque and R. A. Ricci, “Observation of 2.5 MeV neutrons emitted from a titanium-deuterium system,” *Il Nuovo Cimento A* **104** (1991) 1413–1416.

[34] R. Takagi, H. Numata, I. Ohno, K. Kawamura and S. Haruyama, “Neutron emission during a long-term electrolysis of heavy water,” *Fusion Technology* **19** (1991) 2135–2139.

[35] A. Takahashi, T. Takeuchi, T. Iida and M. Watanabe, “Neutron spectra from D_2O–Pd cells with pulse electrolysis,” *AIP Conference Proceedings* **228** (1991) 323–340.

[36] E. Botta, T. Bressani, D. Calvo, A. Feliciello, P. Gianotti, C. Lamberti, M. Agnello, F. Iazzi, B. Minetti and A. Zecchina, “Measurement of 2.5 MeV neutron emission from Ti/D and Pd/D systems,” *Il Nuovo Cimento A* **105** (1992) 1663–1671.

[37] M. Nakada, T. Kusunoki and M. Okamoto, “Energy of the neutrons emitted in heavy water electrolysis,” *Proc. ICCF3* (1993) 173.

[38] M. Bittner, A. Meister, D. Seeliger, R. Schwierz and P. Wüstner, “Observation of dd fusion neutrons during degassing of deuterium-loaded palladium,” *Fusion technology* **23** (1993) 346–352.

[39] H. Q. Long, S. Sun, H. Liu and R. Xie, “Anomalous effects in deuterium/metal systems,” *Proc. ICCF3* (1992) 447.

[40] A. G. Lipson, B. F. Lyakhov, A. S. Roussetski, T. Akimoto, T. Mizuno, N. Asami, R. Shimada, S. Miyashita and A. Takahashi, “Evidence for low-intensity DD reaction as a result of exothermic deuterium desorption from Au/Pd/PdO: D heterostructure,” *Fusion Technology* **38** (2000) 238–252.

[41] B. M. Steinetz, T. L. Benyo, A.Chait, R. C. Hendricks, L. P. Forsley, B. Baramsai, P. B. Ugorowski, M. D. Becks, V. Pines, M. Pines and R. E. Martin, “Novel nuclear reactions observed in bremsstrahlung-irradiated deuterated metals,” *Physical Review C* **101** (2020) 044610.

[42] P. A. Mosier-Boss, S. Szpak, F. E. Gordon and L. P. Forsley, “Triple tracks in CR-39 as the result of PdD Co-deposition: evidence of energetic neutrons,” *Naturwissenschaften* **96** (2009) 135–142.

[43] P. A. Mosier-Boss, J. Y. Dea, L. P. G. Forsley, M. S. Morey, J. R. Tinsley, J. P. Hurley and F. E. Gordon, “Comparison of Pd/D co-deposition and DT neutron generated triple tracks observed in CR-39 detectors,” *The European Physical Journal-Applied Physics* **51** (2010) 20901.

[44] P. A. Mosier-Boss, J. Y. Dea, F. E. Gordon, L. P. Forsley and M. H. Miles, “Review of twenty years of LENR research using Pd/D co-deposition,” *J. Condensed Matter Nuclear Science* **4** (2011) 173–187.

[45] P. A. Mosier-Boss, L. P. G. Forsley, P. Carbonnelle, M. S. Morey, J. R. Tinsley, J. P. Hurley and F. E. Gordon, “Comparison of SEM and optical analyses of DT neutron tracks in CR-39 detectors,” *Radiation Measurements* **47** (2012) 57–66.

[46] J. F. Ziegler, T. H. Zabel, J. J. Cuomo, V. A. Brusic, G. S. Cargill III, E. J. O’Sullivan and A. D. Marwick, A.D., “Electrochemical experiments in cold nuclear fusion,” *Physical Review Letters* **62** (1989) 2929.

[47] K. D. Schilling, P. Gippner, W. Seidel, F. Stary and D. Wohlfarth, “Search for charged-particle emission from deuterated palladium foils,” *Zeitschrift fÃijr Physik A Atomic Nuclei* **336** (1990) 1–4.

[48] V. B. Brudanin, V. M. Bystritsky, V. G. Egorov, S. G. Stetsenko I. A. Yutlandov, “Search for the cold fusion d(d,^{4}He) in electrolysis of D_2O,” *Physics Letters A* **151** (1990) 543–546.

[49] S. E. Jones, F. Keeney, A. Johnson, D. B. Buehler, F. E. Cecil, G. K. Hubler, P. L. Hagelstein, J. Ellsworth and M. Scott, “Charged-particle emissions from metal deuterides,” *Proc. ICCF10* (2003).

[50] R. Taniguchi, T. Yamamoto and S. Irie, “Detection of charged particles emitted by electrolytically induced cold nuclear fusion,” *Japanese Journal of Applied Physics* **28** (1989) L2021.

[51] S. Aiello, F De Filippo, G Lanzanó, S. L. Nigro and A. Pagano, “Nuclear fusion experiment in palladium charged by deuterium gas,” *Fusion technology* **18** (1990) 115–119.

[52] F. E. Cecil, D. Ferg, T. E. Furtak, C. Mader, J. A. McNeil and D. L. Williamson, “Study of energetic charged particles emitted from thin deuterated palladum foils subject to high current densities,” *Journal of Fusion Energy* **9** (1990) 195–197.

[53] F. E. Cecil, H. Liu, D. Beddingfield and C. S. Galovich, “Observation of charged particle bursts from deuterium loaded thin titanium foils,” *AIP Conference Proceedings* **228** (1991) 375–382.

[54] R. Taniguchi, T. Yamamoto and S. Irie, “Fine structure of the charged particle bursts induced by D_2O electrolysis,” *Bull. Univ. Osaka Prefect., Ser A* **39** (1991) 233–240.

[55] W. Mo, Y. S. Liu, L. Y. Zhou, S. Y. Dong, K. L. Wang, S. C. Wang and X. Z. Li, “Search for precursor and charged particles in cold fusion,” *Proc. ICCF2* (1991) 123.

[56] V. A. Tsarev, “Cold fusion studies in the USSR,” *Proc. ICCF3* (1992) 319.

[57] A. B. Karabut, Y. R. Kucherov and I. B. Savvatimova, “Nuclear product ratio for glow discharge in deuterium,” *Physics Letters A* **170** (1992) 265–272.

[58] E. Yamaguchi and T. Nishioka, “Direct evidence for nuclear fusion reactions in deuterated palladium,” *Proc. ICCF3* (1993) 179–188.

[59] R. Taniguchi, “Characteristic peak structures on charged particle spectra during electrolysis experiment,” *Proc. ICCF4* (1994) 18-1.

[60] A. B. Karabut, S. A. Kolomeychenko and I. B. Savvatimova, “High energy phenomena in glow discharge experiments,” *Proc. ICCF5* (1995) 241.

[61] A. G. Lipson, A. S. Roussetski, G. H. Miley and C. H. Castano, “In-situ charged particles and X-ray detection in Pd thin film-cathodes during electrolysis in Li2SO4/H2O,” *Proc. ICCF9* (2002).

[62] A G Lipson, G H Miley, A S Roussetski, and E I Saunin, “Phenomenon of an energetic charged particle emission from hydrogen/deuterium loaded metals,” *Proc. ICCF10* (2003) 539–558.

[63] A S Roussetski, “CR-39 track detectors in cold fusion experiments: Review and perspectives,” *Proc. ICCF11* (2004) 274–280.

[64] A G Lipson, G H Miley, A S Roussetski, B F Lyakhov, and E I Saunin, “Reproducible nuclear emissions from Pd/PdO:Dx heterostructure during controlled exothermic deuterium desorption,” *Proc. ICCF12* (2005) 293–313.

[65] A. Kitamura, Y. Sasaki, Y. Miyoshi, A. Taniike, A. Takahashi, R. Seto and Y. Fujita, “Heat evolution from Pd nano-powders exposed to high-pressure hydrogen isotopes and associated radiation measurements,” *J. Condensed Matter Nuclear Science* **4** (2011) 56.

[66] P. A. Mosier-Boss, L. Forsley and P. McDaniel, “The Use of CR-39 Detectors in LENR Experiments,” *J. Condensed Matter Nuclear Science* **14** (2014) 29.

[67] E. Lukosi, M. A. Prelas, J. Shim, H. Kasiwattanawut, C. Weaver, C. Mathai, S. Gangopadhyay and K. Preece, “Diamond-based radiation sensor for LENR experiments. Part 2: Experimental analysis of deuterium-loaded palladium,” *J. Condensed Matter Nuclear Science* **13** (2014) 329.

[68] C. Weaver, M Prelas, H. Kasiwattanawut, J. Shim, M. Watermann, C. J. Mathai, S. Gangopadhyay and E. Lukosi, “Progress in development of diamond-based radiation sensor for use in LENR experiments,” *J. Condensed Matter Nuclear Science* **15** (2015) 305.

[69] D. Zhou, C. Wang, Y. Sun, J. B. Liang, G. Zhu, L. Forsley, X. Z. Li, P. A. Mosier-Boss and F. Gordon, “Energetic particles generated in earlier Pd + D nuclear reactions,” *J. Condensed Matter Nuclear Science* **15** (2015) 33.

[70] E. Ziehm, *An experimental investigation of low energy nuclear reactions in a DC glow discharge* PhD Thesis UIUC (2022).

[71] "Experiment 4: Alpha spectroscopy with silicon charged-particle detectors," Ortec/Ametek.

[72] P. L. Hagelstein, "Possibility of coherent LENR dynamics with nuclear molecules," to appear in *J. Condensed Matter Nuclear Science*.

[73] Z. Sun and D. Tomanek, "Cold fusion: How close can deuterium atoms come inside palladium," *Phys. Rev. Lett.* **63** (1989) 59.

[74] O. B. Christensen, P. D. Ditlevsen, K. W. Jacobsen, P. Stolze, O. H. Nielsen and J. K. Norskov, "H–H interactions in Pd," *Phys. Rev. B* **40** (1989) 1993.

[75] S.-H. Wei and A. Zunger, "Instability of diatomic deuterium in fcc palladium," *J. Fusion Energy* **9** (1990) 367.

[76] P. Nordlander, J. K. Norskov, F. Besenbacher and S. M. Myers, "Multiple deuterium occupancy of vacancies in Pd and related metals," *Phys. Rev. B* **40** (1989) 1990.

[77] P. L. Hagelstein, "Molecular D_2 near vacancies in PdD and related problems," *J. Condensed Matter Nuclear Science* **13** (2014) 138.

[78] C. Jarque and O. Navaro, M. E. Ruiz and J. Garcia-Prieto, "On the stability of the PdH_2 molecule," *J. American Chemical Society* **108** (1986) 3507.

[79] O. Novaro and C. Jarque, "Potential energy surface for the Pd-H_2 system: Comparison with matrix isolation experiments," *Theor. Chim. Acta* **80** (1991) 19.

[80] L. Andrews, L. Manceron, M. E. Alikhani and X. Wang, "Observed and calculated infrared spectrum of Pd(H_2) in solid argon: A ligand-free side-bonded molecular hydrogen complex," *J. American Chemical Society* **122** (2000) 11011.

[81] M. R. A. Blomberg and P. E. M. Siegbahn, "An important bound singlet state of NiH_2," *J. Chem. Phys.* **78** (1983) 986.

[82] J. A. Platts, "Theoretical electron densities in transition metal dihydrides," *Journal of Molecular Structure (Theochem)* **545** (2001) 111.

[83] L. Andrews, "Matrix infrared spectra and density functional calculations of hydrides and dihydrogen complexes," *Chem. Soc. Rev.* **33** (2004) 123.

[84] P. L. Hagelstein, "Models based on phonon-nuclear coupling," *Cold Fusion: Advances in Condensed Matter Nuclear Science*, J. P. Biberian, editor, Elsevier (2020) 283–300.

[85] A. Khellaf, R. M. Emrick, and J. J. Vuillemin, "Slow quenches of high-quality single crystals of platinum and palladium," *Physical Review B* **37** 6717.

[86] T. R. Mattsson and A. E. Mattsson, "Calculating the vacancy formation energy in metals: Pt, Pd, and Mo," *Physical Review B* **66** (2002) 214110.

[87] J. E. Worsham Jr, M. K. Wilkinson and C. G. Shull, "Neutron-diffraction observations on the palladium-hydrogen and palladium-deuterium systems," *Journal of Physics and Chemistry of Solids* **3** (1957) 303–310.

[88] F. Besenbacher, J. Böttiger and S. M. Myers, "Defect trapping of ion-implanted deuterium in nickel," *Journal of Applied Physics* **53** (1982) 3536–3546.

[89] F. Besenbacher, B. B. Nielsen, J. K. Norskov, S. M. Myers and P. Nordlander, "Interaction of hydrogen isotopes with metals: Deuterium trapped at lattice defects in palladium," *Journal of Fusion Energy* **9** (1990) 257–261.

[90] J. Mao and R. B. McClellan, "Vacancy concentrations in metals in equilibrium with H_2 at high pressures," *Journal of Physics and Chemistry of Solids* **64** (2003) 527.

[91] Y. Fukai and N. Okuma, "Formation of superabundant vacancies in Pd hydride under high hydrogen pressures," *Phys. Rev. Lett.* **73** (1994) 1640.

[92] Y. Fukai, M. Mizutani, S. Yokota, M. Kanazawa, Y. Miura and T. Watanabe, "Superabundant vacancy-hydrogen clusters in electrodeposited Ni and Cu," *Journal of Alloys and Compounds* **356-357** (2003) 270.

[93] S. Szpak, P. A. Mosier-Boss and J. J. Smith, "On the behavior of Pd deposited in the presence of evolving deuterium," *J. Electroanalytical Chemistry* **302** (1991) 255.

[94] P. L. Hagelstein and I. U. Chaudhary, "Arguments for dideuterium near monovacancies in PdD," *Proc. ICCF15* (2009) 282–287.

[95] D. Letts, "Codeposition methods: A search for enabling factors," *J Condensed Matter Nuclear Science* **4** (2011) 81.

[96] D. Letts and P. L. Hagelstein, "Modified Szpak protocol for excess heat," *J Condensed Matter Nuclear Science* **6** (2012) 44.

[97] S. Szpak, P. A. Mosier-Boss and F. E. Gordon, "Further evidence of nuclear reactions in the Pd/D lattice: emission of charged particles," *Naturwissenschaften* **94** (2007) 511–514.

[98] P. A. Mosier-Boss, L. P. G. Forsley and P. K. McDaniel, *Investigation of nano nuclear reactions in condensed matter*, DTRA Final Report (2016).

[99] P. A. Mosier-Boss, F. E. Gordon, L. P. Forsley and D. Zhou, "Detection of high energy particles using CR-39 detectors Part 1: Results of microscopic examination, scanning, and LET analysis," *Int. J Hydrogen Energy* **42** (2017) 416.

[100] M. C. H. McKubre, S. Crouch-Baker, M. C. Rocha-Filho, S. I. Smedley, F. L. Tanzella. T. O. Passell and J. Santucci, "Isothermal flow calorimetric investigations of the D/Pd and H/Pd systems," *J. Electroanalytical Chemistry* **368** (1994) 55.

[101] P. L. Hagelstein, "Bird's eye view of phonon models for excess heat in the Fleischmann-Pons experiment," *J Condensed Matter Nuclear Science* **5** (2012) 169.

[102] M. McKubre, F. Tanzella, P. L. Hagelstein, K. Mullican and M. Trevithick, "The need for triggering in cold fusion reactions," *Proc. ICCF10* (2003) 199–212.

[103] F. Tanzella, J. Bao, M. McKubre and P. Hagelstein, "Stimulation of metal deuteride wires at cryogenic temperatures," *J Condensed Matter Nuclear Scienc* **12** (2012) 176–186.

[104] E. Yamaguchi and T. Nishioka, "Cold nuclear fusion induced by controlled out-diffusion of deuterium in palladium," *Japanese Journal of Applied Physics, Part 2* **29** (1990) L666.

[105] E. Yamaguchi and T. Nishioka, "Nuclear fusion induced by the controlled out-transport of deuterons in palladium," *AIP Conference Proceedings* **228** (1991) 324.
[43] A. G. Lipson, G. H. Miley, A. S. Roussetski and E. I. Saunin, Phenomenom of an energetic charged particle emission from hydrogen/deuterium loaded metals, Proc ICCF10 (2003). (Available from LENR-CANR.org)

[106] J. H. Elliot, "Thick junction radiation detectors made by ion drift," *Nuclear Instruments and Methods* **12** (1961) 60–66.

[107] B. D. Wilkins, M. J. Fluss, S. B. Kaufman, C. E. Gross and E. P. Steinberg, "Pulse-height defects for heavy ions in a silicon surface-barrier detector," *Nuclear Instruments and Methods* **92** 381–391.

[108] J. F. Ziegler, "SRIM-2003," *Nuclear instruments and methods in physics research section B: Beam interactions with materials and atoms* **219** (2004) 1027–1036.

[109] J. Barreto, L. Tassan-Got, C. Stephan, J. P. Garron and M. Langevin, "Absence of closed shell effect in the fusion reaction ^{40}Ca+^{48}Ca at 330 MeV," *Physical Review C* **25** 1641.

[110] J. Barreto, G. Auger, M. Langevin and E. Plagnol, "Fusion of the ^{40}Ca+^{40}Ca system," *Physical Review C* **27** 1335.

[111] J. W. Engle, G. W. Severin, T. E. Barnhart, L. D. Knutson and R. J. Nickles, "Cross sections of the ^{36}Ar(d,α)^{34m}Cl, ^{40}Ar(d,α)^{38}Cl, and ^{40}Ar(d,p)^{41}Ar nuclear reactions below 8.4 MeV," *Applied Radiation and Isotopes* **70** (2012) 355–359.

[112] A. J. Koning, D. Rochman, J. C. Sublet, N. Dzysiuk, M. Fleming and S. Van der Marck, "TENDL: complete nuclear data library for innovative nuclear science and technology," *Nuclear Data Sheets* **155** (2019) 1–55.

[113] H. O. Menlove, M. M. Fowler, F. Garcia, M. C. Miller, M. A. Paciotti, R. R. Ryan and S. E. Jones, "Measurement of neutron emission from Ti and Pd in pressurized D_2 gas and D_2O electrolysis cells," *Journal of Fusion Energy* **9** (1990) 495–506.

[114] K. Mizuno, Y. Furuya, K. Hirano and H. Okamoto, "Hydrogen diffusion in titanium-hydride observed by the diffraction-enhanced X-ray imaging method," *Physica Status Solidi (a)* **204** (2007) 2734–2739.